Carpathian Journal of Earth and Environmental Sciences, May 2014, Vol. 9, No. 2, p. 71 - 78

NEW OCCURRENCES OF HESSITE, PETZITE AND STÜTZITE AT CORANDA-HONDOL OPEN PIT (CERTEJ GOLD-SILVER DEPOSIT, ROMANIA)

Andrei Ionut APOPEI[1,*], Gheorghe DAMIAN[1,2], Nicolae BUZGAR[1], Stanislava MILOVSKA[3] & Andrei BUZATU[1]

*[1]"Alexandru Ioan Cuza" University of Iaşi, Faculty of Geography and Geology, Department of Geology, 20A Carol I Blv., 700505 Iaşi, Romania, *e-mail: andrei_ionut1987@yahoo.com*

[2]Tech Univ Cluj Napoca, North University Center of Baia Mare, 62A Dr. Victor Babeş Street, 430083 Baia Mare, Romania.

[3]Geological Institute, Slovak Academy of Sciences, Severná 5, 974 01 Banská Bystrica, Slovakia.

Abstract: Au-Ag- and Ag-tellurides are widely abundant in the vast majority of the "Golden Quadrilateral" (Metaliferi Mts., Romania) ore deposits. Optical microscope observations, electron microprobe and μ-Raman analyses have been successfully carried out to identify Au-Ag-Te minerals from Coranda-Hondol open pit (part of Certej deposit, South Apuseni Mountains, in Romania). The identified tellurides are hessite (Ag_2Te), petzite (Ag_3AuTe_2) and stützite ($Ag_{5-x}Te_3$, where x = 0.24-0.36) and they usually occur as patches (reaching 90-100 μm in length) in galena, bournonite-seligmannite or at the contact between the last three minerals. In general, all the microanalytical data are stoichiometric with a slightly compositional variation in the case of hessite. The μ-Raman spectrum of stützite shows a characteristic Raman fingerprint with a very strong band at 147 cm^{-1}. The broadness of the Raman band (147 cm^{-1}) indicates a non-homogeneous distribution and, in conjunction with the strong heterogeneity observed under microscope, it suggests that the tellurides have formed contemporaneously and they can possibly be attributed to a later silver-rich telluride-bearing substage.

Keywords: Certej, Coranda-Hondol, tellurides, hessite, petzite, stützite, EPMA, Raman spectroscopy

1. INTRODUCTION

The "Golden Quadrilateral" (Metaliferi Mts., Romania) is well-known for the telluride-bearing epithermal ore deposits (Ciobanu et al., 2004b; Cook & Ciobanu, 2004; Cook et al., 2004).

Besides the economic interest of Au-Ag tellurides they bare, they are also a good indicator of gold (also known as gold carrier) (Ciobanu et al., 2004b; Tamas et al., 2006; Maslennikov et al., 2012).

By far, the most important deposit of Au-Ag- and Ag-tellurides from the "Golden Quadrilateral" is the Săcărîmb ore deposit, where the Au/Te ratio is 1:2 (Udubașa & Udubașa, 2004). Also, many tellurides have been described for the first time in the world at the Săcărîmb ore deposit (e.g. nagyágite, petzite, stützite, museumite, etc.) (Bindi & Cipriani, 2004; Ciobanu et al., 2004a).

The Au-Ag- and Ag-tellurides are generally less abundant in other deposits from the "Golden Quadrilateral", *i.g.* Brad (Musariu), Fața Băii – Larga (Horia level, 516 m), Baia de Arieș, etc. (Cook et al., 2004).

To the best of our knowledge, only one telluride, i.e. kostovite ($CuAuTe_4$) was mentioned at the Coranda-Hondol open pit, but its presence was not confirmed by any analytical technique (Udubasa et al., 1992).

The current study presents new occurrences and compositional data on the Au-Ag- and Ag-tellurides from Coranda-Hondol open pit. The hessite (Ag_2Te), petzite (Ag_3AuTe_2) and stützite ($Ag_{5-x}Te_3$, where x = 0.24-0.36) were identified by means of EPMA (Electron Probe Microanalyzer) and Raman spectroscopy techniques. Also, the presence of these tellurides was optically and texturally characterized. Furthermore, the temperature conditions regarding the formation of

these ternary assemblages hessite-petzite-stützite are taken into discussion.

2. GEOLOGY

The Coranda-Hondol open pit (CHOP) is located at the southern extremity of the "Golden Quadrilateral", South Apuseni Mountains (45° 59' 37'' N, 23° 00' 27'' E, Metaliferi Mts., Romania). This area was mined for gold and silver (late 17th century) and it recently hosted operations focused mainly on the extraction of Pb and Zn. The ore from CHOP is part of the Certej metalliferous ore deposit.

The main metalliferous minerals from the CHOP are galena (PbS), Fe-poor sphalerite (Zn,Fe)S (1-3% Fe, Udubașa et al., (1982) and pyrite (Fe_2S). Chalcopyrite ($CuFeS_2$) and sulfosalts occur only at microscopic level. Chalcopyrite mainly occurs as "chalcopyrite disease" in sphalerite. The gangue minerals (of no economic value) are quartz, calcite, rhodocrosite, barite and adularia (potassium aluminosilicate).

Several reviews have described the geological setting and geology of the Coranda-Hondol open pit (Ianovici et al., 1976; Udubașa et al., 1982; Alderton et al., 1998; Pricopie et al., 2004; Ageneau et al., 2006; Forward et al., 2009; Apopei et al., 2012).

3. MATERIALS AND METHODS

The samples were randomly collected from the entire perimeter of the Coranda-Hondol open pit. The telluride minerals usually occur as patches which can reach 100 μm in size and only grains larger than 10-20 μm were could be observed at a magnification up to 20X. Most probably there are other grains which contain one or more telluride minerals, but they are observable only at high magnification as it is the case of point 6 (hessite, observed during EPMA analyses) from figure 1g.

The identity of the telluride minerals has been established firstly based on their optical properties, and then it was confirmed by EPMA and in the case of stützite by micro Raman measurement.

An optical microscope MEIJI ML9430 was used for the optical observations in reflected light (air technique), having a DSLR camera (Canon® 450D) attached to it for the microphotographs.

The mineral phases were analyzed on a Cameca SX-100 Electron Probe Microanalyzer (EPMA), at the State Geological Institute of Dionyz Stur (Bratislava), equipped with one ED (energy-dispersive) and four WD (wavelength-dispersive) spectrometers. All the measurements were performed on carbon coated polished sections using an acceleration voltage of 25 kV, 4 μm beam diameter and the following lines and standards: S *K*α ($CuFeS_2$), Fe *K*α ($CuFeS_2$), Pb *M*α (PbS), Cu *K*α (Cu), Ag Lα (Ag), As *K*α, *L*α (GaAs), Sb *L*β (Sb), Se *L*β (Bi_2Se_3), Te *L*α (Bi_2Te_3), Hg *L*α (HgS), Bi *L*α (Bi), Zn *K*α (ZnS), Mn *K*α (Mn), Au *L*α (Au).

The non-polarized micro-Raman spectrum was obtained using a Horiba - Jobin Yvon - Labram spectrometer, equipped with an Olympus microscope. The 632.81 nm line of a He-Ne laser was used as excitation, 600 lines/mm holographic grating and CCD detector were used. The instrument includes confocal mode system. The laser power was controlled by means of a series of density filters in order to avoid heating effects.

4. RESULTS AND DISCUSSIONS

4.1. Optical and textural features

The polished section (sample number CH06/3A) was studied firstly by using an optical microscope in reflected light (air technique) at magnification up to 20X. In plane-polarized incident light the hessite (Ag_2Te) is grey with slightly brownish tint, scratches, while in crossed nicols it shows a dark orange and bluish distinct anisotropy (see Fig. 1b, 1c, 1c1 and 1h). At this magnification of the microscope (20X) the optical differences between hessite and petzite (Ag_3AuTe_2) are unnoticeable (Cabri, 1965; Pracejus, 2008).

Ag- and/or Au-Ag-tellurides usually occur as patches (Fig. 1d, 50-100 μm in size) in galena (Gn), in bournonite-seligmanite (Bnn-Slg) (Fig. 1g, 10 μm in size) and at the contact between galena and bournonite-seligmanite (Figure 1c and 1c1, 80 μm in size). Ag- and/or Au-Ag-tellurides can also be observed inside sulfosalts (bournonite-seligmanite) veins (Fig. 1h, 5-10 μm in width and 30 μm long).

4.2. Electron microprobe analyses

Electron microprobe analyses reveal the presence of hessite and petzite. Based on the results of the chemical composition (Table 1), the content of Ag and Te in hessite is from 57.35 wt.% to 60.61 wt.% and from 35.77 wt.% to 38.35 wt.%, respectively. For petzite, the content of Ag, Te and Au is 41.90 wt.% to 42.07 wt.%, 29.88 wt.% to 32.31 wt.% and 22.74 wt.% to 23.91 wt.%, respectively. The empirical formulas calculated on the basis of the total number of atoms are shown in table 1. The microanalytical data give the empirical mean composition $Ag_{3.06}Au_{0.93}(Te_{1.92}Se_{0.05}S_{0.01})_{\sum=1.98}$ for petzite, and $Ag_{1.96}Te_{1.02}$ for hessite.

Table 1. Electron microprobe analyses of Au-Ag tellurides from the Certej deposit (Coranda-Hondol open pit) (wt.%).

sample point #	Analysis (wt.%)											Calculated formula	Mineral
	S	Pb	Ag	Cu	As	Sb	Fe	Se	Te	Hg	Bi	Au	Total		
p1	0.03	0	60.61	0	0.21	0	0	0	36.43	0.02	0	0.04	97.33	$(Ag_{1.98}As_{0.01})_{\Sigma=1.99}Te_{1.01}$	Hessite
p2	0.02	0	60.24	0	0.06	0	0	0.06	35.95	0.06	0.04	0.03	96.47	$Ag_{1.99}Te_{1.00}$	Hessite
p3	0.05	0	60.59	0	0.07	0	0	0.08	35.77	0	0.03	0.05	96.64	$Ag_{1.99}(Te_{0.99}S_{0.01})_{\Sigma=1.00}$	Hessite
p4	0.09	0	42.07	0	0.02	0	0	0.61	29.88	0.01	0	23.91	96.59	$Ag_{3.09}Au_{0.96}(Te_{1.86}Se_{0.06}S_{0.02})_{\Sigma=1.94}$	Petzite
p5	0.07	0	41.90	0	0.12	0	0	0.53	32.31	0.04	0	22.74	97.71	$Ag_{3.04}Au_{0.90}(Te_{1.98}Se_{0.05})_{\Sigma=2.03}$	Petzite
p6	0.12	0	57.35	0	0.10	0	0	0.03	38.35	0.01	0	0.09	96.05	$Ag_{1.90}(Te_{1.08}S_{0.01})_{\Sigma=1.09}$	Hessite

Empirical formulaes were calculated on the basis of total atoms (3 for hessite and 6 for petzite).

Most of the compositions of hessite from the Coranda-Hondol open pit are close to stoichiometric composition, with one exception. This grain shows a slight depletion in Ag and enrichment in Te (p6, Table 1, Fig. 1g). The silver and tellurium contents of hessite range from 57.35 to 60.61 wt.%, respectively from 35.77 to 38.35 wt.%. In the Au-Ag-Te diagram this compositional variation (sample point 6, Table 1) was plotted between the theoretical composition of hessite and stützite (see Fig. 2b). In the case of petzite, the compositional variation shows a slight depletion in Te. The tellurium contents of petzite range from 32.31 (which is close to stoichiometric content) to 29.88 wt.%. Minor compositional variations of Ag and Au can be observed (Table 1).

Figure 2. Ternary Au-Ag-Te diagram (atomic proportions) for mineral compositions analyzed in the present study (white circles) and for theoretical compositions of other associated Au-Ag tellurides (black circles)

The atomic percents of Au, Ag and Te are plotted in the ternary Au-Ag-Te diagram (Fig. 2). The plotted points filled with white color correspond to experimental data from this study, while the points filled with black color correspond to other Ag- and/or Au-Ag-tellurides of the system Au-Ag-Te.

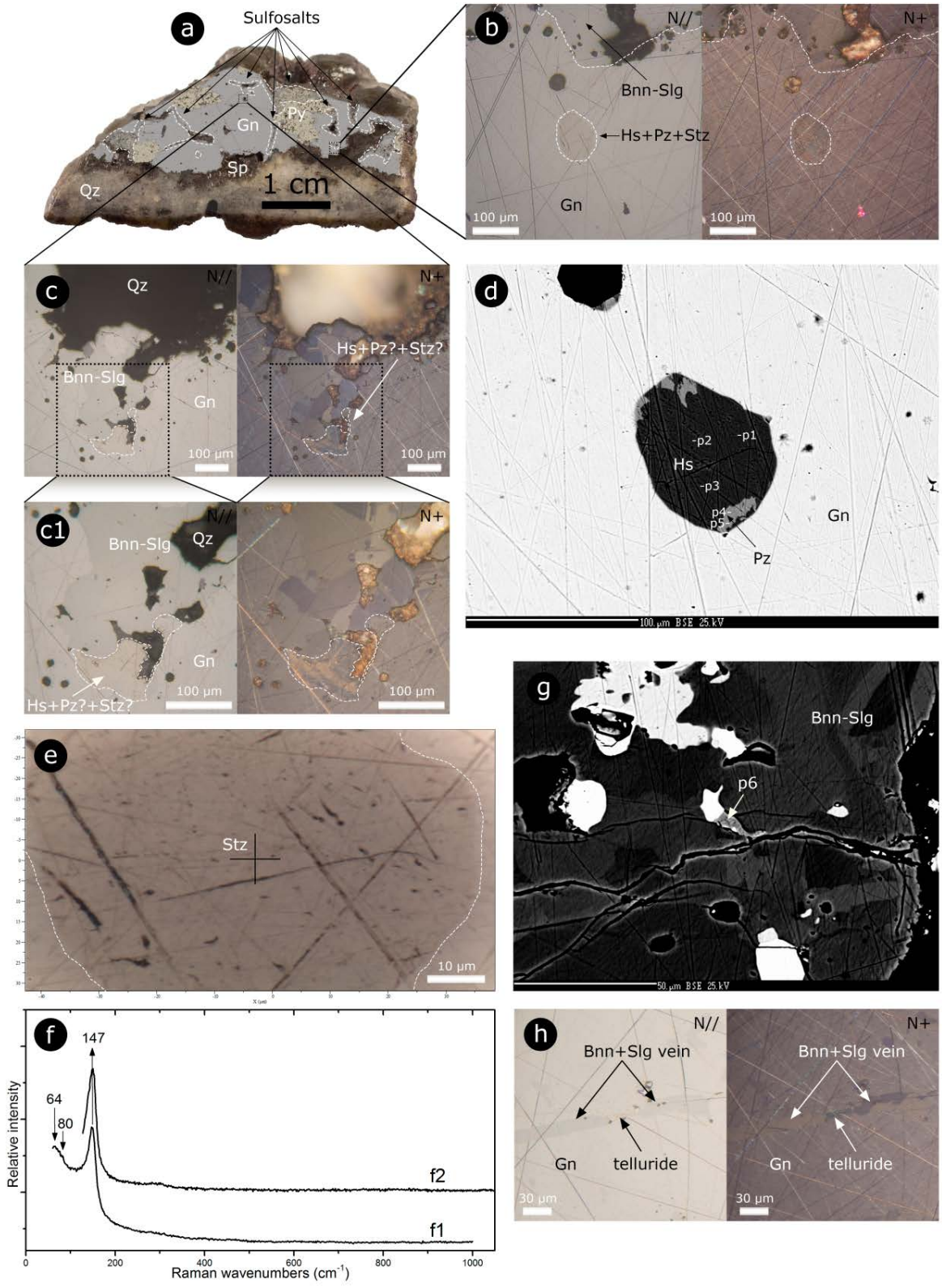

Figure 1. a) Polished section with quartz (Qz), galena (Gn), pyrite (Py), sphalerite (Sph) and veins of sulphosalts in galena; b) c) c1) Reflected light microphotographs (left – plane polarized light; right – cross polarised light) demonstrating the presence of telluride minerals found as inclusion in galena (Gn) and at the contact with bournonite-seligmanite (Bnn-Slg) and quartz (Qz); d) Back-scattered electron image (BEI) of petzite (Pz) found as inclusions in hessite (Hs); e) The crosshair marked in black is the spot was the micro-Raman spectrum of stützite (Stz) (Figure 1f, spectrum f1) was acquired and compared with reference R070701 (spectrum f2), (Downs, 2006); g) Back-scattered electron image (BEI) of hessite (Hs) found as inclusion in bournonite-seligmanite (Bnn-Slg); and h) Au-Ag-Te minerals in the veined sulfosalts (Bnn-Slg).

The solid lines represent the observed assemblage (hessite-petzite-stützite) in the Coranda-Hondol deposit, in terms of the system Au-Ag-Te. The dotted lines represent the inferred assemblages in the system Au-Ag-Te based on the association hessite-petzite-stützite and considering the ternary system (Cabri, 1965) and the binary system silver-tellurium (Kracek et al., 1966; Karakaya & Thompson, 1991).

4.3. μ-Raman spectroscopy

The Raman spectrum of petzite could not be acquired due to the small size of the grains of this mineral. Due to the fact that the sample was polished in order to remove the thin layer of carbon, the Raman spectrum acquired from the area does not correspond to hessite as it was first belived based on EPMA analyses, but it reveals the presence of stützite ($Ag_{5-x}Te_3$, where x = 0.24-0.36). The stützite, hessite and petzite are intergrown irregularly, suggesting the contemporaneous formation (Burbank & Henderson, 1932).

The Raman spectrum of stützite is shown in the figure 1, spectrum f1, and it was compared with the reference standard (Fig. 1, spectrum f2, R070701, with the measured chemistry $Ag_{4.94}Te_{3.00}$, Downs (2006)). The Raman spectrum of stützite is in good agreement with the Raman spectrum of synthetic $Ag_{5-x}Te_3$ (stützite) (Milenov et al., 2013).

According to the group theory classification (Aroyo et al., 2006a; Aroyo et al., 2006b), the full vibrational representations of $Ag_{5-x}Te_3$ (stützite) contain $\Gamma = 9A_{1g} + 3A_{1u} + 6A_{2g} + 10A_{2u} + 6B_{1g} + 8B_{1u} + 5B_{2g} + 8B_{2u} + 11E_{2u} + 15E_{2g} + 18E_{1u} + 11E_{1g}$ modes (space group *P*6/*mmm* (No. 191) and its point group D_{6h} (6/mmm), crystal structure from Downs and Hall-Wallace (2003)). The representation may be reduced to $9A_{1g} + 15E_{2g} + 11E_{1g}$ Raman active modes.

The Raman peak centered at 147 cm^{-1} (tentatively assigned to E_g vibration) with the full width at a half maximum (FWHM) around 20 cm^{-1} is the distinguishable feature for the stützite against that of hessite. Unfortunately, the notch filter cuts the wavelengths below 60 cm^{-1}. At these low wavelengths, a Raman peak can be observed at 64 cm^{-1} with a shoulder located at 80 cm^{-1} (tentatively assigned to A_g vibrations). There were no other Raman peaks in the higher frequency spectral domain (over 200 cm^{-1}) of the stützite. The broadness of the band centered at 147 cm^{-1} indicates the non-homogeneous distribution.

In the case of the Raman spectrum of hessite two strong peaks arise at 119 cm^{-1} and 138 cm^{-1} (R060226, Downs (2006)). The Raman bands observed in the present study and those characteristic bands of stützite, hessite and petzite are summarized in Table 2.

4.4. Formation of hessite, petzite and stützite

Taking into account the strong heterogeneity (varying from dark orange to dark bluish grey in crossed nicols) under the microscope (see figure 1b, 1c and 1c1), the hessite is monoclinic rather than cubic (Xu et al., 2012). Also, it may be pointed out that hessite is formed bellow 145±3 °C, because the transition of hessite from monoclinic to cubic (fcc, face-centered cubic) occurs at this temperature (Cabri, 1965; Kracek et al., 1966; Karakaya & Thompson, 1991).

Table 2. Raman bands, comparison between stützite, hessite, petzite and observed Raman peaks in this study.

This	stützite		hessite		petzite
study	†	‡	†	‡	†
64^{vw}	n/a	n/a	n/a	n/a	n/a
80^{sh}	n/a	n/a	n/a	n/a	n/a
-	n/a	-	**119^{vs}**	**110^{vs}**	n/a
147^{vs}	**147^{vs}**	**151^{br}**	**138^{vs}**	**138^{vs}**	n/a
-	-	-	-	-	**163^{vs}**
-	-	-	-	-	174^{m}
-	-	-	-	-	~320^{m}

Notes: † Downs (2006), ‡ Milenov et al., (2013) (synthetic); ^{vs}very strong; ^{s}strong; ^{m}medium; ^{w}weak; ^{vw}very weak; ^{sh}shoulder; ^{br}broad; n/a - not applicable (the wavelengths are missing).

Furthermore, the intergrowths between hessite-petzite-stützite may be a breakdown product of the chi(χ)-phase (below 50±20°C) and/or a decomposition of the gamma(γ)-phase (below 120±15°C) (Kiukkola & Wagner, 1957; Cabri, 1965; Afifi et al., 1988; Ciobanu et al., 2004a). Echmaeva & Osadchii (2009) confirm the γ-phase decomposition reactions by electromotive force (EMF) method, which form a mixture of hessite and stützite.

Similar assemblages involving Ag- and/or Au-Ag-tellurides are discussed previously, e.g. stützite-hessite-petzite and hessite-stützite in Colorado (Honea, 1964), hessite-petzite-stützite in Emperor (Pals & Spry, 2003), petzite-hessite-stützite in Săcărîmb (Ciobanu et al., 2004a) and hessite-petzite or hessite-petzite-sylvanite in Roșia Montană (Ciobanu et al., 2004b).

Obviously, these assemblages do not represent the initial conditions of ore-formation but rather a

re-equilibration during cooling. Acoording to the previous discussions and taking into account the phase relations of Cabri (1965), the assemblage of hessite-petzite-stützite forms due to the breakdown of a mixture between χ-phase and γ-phase at temperatures bellow 120±15 °C.

The observations made regarding the Au-Ag- and/or Ag- tellurides assemblages from the Coranda-Hondol open pit suggest the contemporaneous formation. This can be separated into at least two substages: (i) an early gold-rich telluride-bearing substage and (ii) a later silver-rich telluride-bearing substage dominated by hessite and subordinated amounts of petzite and stützite. The presence of the early gold-rich telluride-bearing substage is still questionable and more analytical and optical observations need to be made to that effect. These assumptions imply the existence of another assemblage consisting of ?calaverite-?krennerite-?sylvanite, ?krennerite-petzite, ?sylvanite-hessite and/or ?sylvanite-petzite (see the inferred tie lines in figure 2a).

5. CONCLUSIONS

Ag- and/or Au-Ag-tellurides (hessite, petzite and stützite) are identified for the first time at the Coranda-Hondol open pit.

Optical and textural observations are accompanied by EPMA and μ-Raman analysis for identification purpose. The μ-Raman spectrum of stützite shows a distinct fingerprint against hessite, petzite or other Ag- and/or Au-Ag-telluride. The broadness of the main Raman peak of stützite (147 cm^{-1}) may be related to the non-homogeneous distribution.

The Ag- and/or Au-Ag-telluride are represented by hessite with subordinated amounts of petzite and stützite. They usually occur as patches in galena, bournonite-seligmanite and at the contact between galena and bournonite-seligmanite series.

The microscopic observations and the presence of the intergrowths of hessite, petzite and stützite may be related to the breakdown of a mixture between χ-phase and γ–phase of ternary Au-Ag-Te solution, bellow 120±15 °C.

The observations of the hessite-petzite-stützite assemblage at the Coranda-Hondol open pit suggest that they have formed contemporaneously and that they can possibly be attributed to a later silver-rich telluride-bearing substage.

Further investigations are however necessary to interpret the presence of other assemblages (?calaverite-?krennerite-?sylvanite, ?krennerite-petzite, ?sylvanite-hessite and/or ?sylvanite-petzite) which probably belong to a gold-rich telluride-bearing substage preceded by the later silver-rich telluride-bearing substage.

6. ACKNOWLEDGEMENTS

The authors gratefully acknowledge the staff of S.C. DevaGold S.A. for access on the Coranda-Hondol open pit and their support on the sampling site. Special thanks go to Dr. Peter Andráš from the Geological Institute of the Slovak Academy of Sciences for the facilitating of the microprobe analyses. Thanks are also extended to the staff of the laboratory of electron microanalysis (from the State Geological Institute of Dionýz Štúr): Dr. Konečný Patrik, Dr. Ivan Holický and Dr. Viera Kollárová for the EPMA analyses.

REFERENCES

Afifi, A.M., Kelly, W.C., & Essene, E.J., 1988. *Phase relations among tellurides, sulfides, and oxides; I, Thermochemical data and calculated equilibria.* Economic Geology, 83(2), 377-394.

Ageneau, M., Mastrodicasa, L., & Marton, I., 2006. *Magmatism and metallogeny of the Certej-Săcărâmb District, Apuseni Mts.* Romania Field Trip SEG Student Chapters Uni Geneva - ETH Zürich - Uni Budapest - Uni Cluj.

Alderton, D.H.M., Thirlwall, M.F., & Baker, J.A., 1998. *Hydrothermal alteration associated with gold mineralization in the southern Apuseni mountains, Romania: preliminary Sr isotopic data.* Mineralium Deposita, 33, 520-523.

Apopei, A.I., Damian, G., & Buzgar, N., 2012. *A preliminary Raman and FT-IR spectroscopic study of secondary hydrated sulfate minerals from the Hondol open pit (Metaliferi Mts., ROMANIA).* Romanian Journal of Mineral Deposits, 85(2), 1-6.

Aroyo, M.I., Kirov, A., Capillas, C., Perez-Mato, J., and Wondratschek, H., 2006a. *Bilbao Crystallographic Server. II. Representations of crystallographic point groups and space groups.* Acta Crystallographica Section A: Foundations of Crystallography, 62(2), 115-128.

Aroyo, M.I., Perez-Mato, J.M., Capillas, C., Kroumova, E., Ivantchev, S., Madariaga, G., Kirov, A., and Wondratschek, H., 2006b. *Bilbao Crystallographic Server: I. Databases and crystallographic computing programs.* Zeitschrift für Kristallographie, 221(1/2006).

Bindi, L., & Cipriani, C., 2004. *Museumite, $Pb_5AuSbTe_2S_{12}$, a new mineral from the gold-telluride deposit of Sacarîmb, Metaliferi Mountains, western Romania.* European Journal of Mineralogy, 16(5), 834-837.

Burbank, W.S., & Henderson, C.W., 1932. *Geology and ore deposits of the Bonanza mining district, Colorado, with a section on history and production.* U.S. Geological Survey, Professional Paper, 169.

Cabri, L.J., 1965. *Phase relations in the Au-Ag-Te systems and their mineralogical significance.* Economic Geology, 60(8), 1569-1606.

Ciobanu, C.L., Cook, N.J., Damian, G., Damian, F. & Buia, G., 2004a. *Telluride and sulphosalt associations at Sacaramb. In N.J. Cook, Ciobanu, C.L., Ed. Au-Ag-telluride Deposits of the Golden Quadrilateral, Apuseni Mts., Romania.*, Guidebook of the International Field Workshop of IGCP Project 486, IAGOD Guidebook Series, Alba Iulia, Romania.

Ciobanu, C.L., Cook, N.J., Tămaș, C., Leary, S., Manske, S., O'Connor, G. & Minut, A., 2004b. *Tellurides-gold-base metal associations at Roșia Montană: the role of hessite as gold carrier.* In N.J. Cook, Ciobanu, C.L., Ed. Au-Ag-telluride Deposits of the Golden Quadrilateral, Apuseni Mts., Romania., Guidebook of the International Field Workshop of IGCP Project 486, IAGOD Guidebook Series, p. 187-202, Alba Iulia, Romania.

Cook, N.J., and Ciobanu, C.L., 2004. *Bismuth tellurides and sulphosalts from the Larga hydrothermal system, Metaliferi Mts, Romania: Paragenesis and genetic significance.* Mineralogical Magazine, 68(2), 301-321.

Cook, N.J., Ciobanu, C.L., Damian, G., & Damian, F., 2004. *Tellurides and sulphosalts from deposits in the Golden Quadrilateral*. In N.J. Cook, Ciobanu, C.L., Ed. Au-Ag-telluride Deposits of the Golden Quadrilateral, Apuseni Mts., Romania., Guidebook of the International Field Workshop of IGCP Project 486, IAGOD Guidebook Series, p. 111-144, Alba Iulia, Romania.

Downs, R.T., 2006. *The RRUFF Project: an integrated study of the chemistry, crystallography, Raman and infrared spectroscopy of minerals.* Program and Abstracts of the 19th General Meeting of the International Mineralogical Association in Kobe, Japan. O03-13.

Downs, R.T., & Hall-Wallace, M., 2003. T*he American Mineralogist crystal structure database*. American Mineralogist, 88(1), 247-250.

Echmaeva, E.A., & Osadchii, E.G., 2009. Determination of the thermodynamic properties of compounds in the Ag-Au-Se and Ag-Au-Te systems by the EMF method. Geology of Ore Deposits, 51(3), 247-258.

Forward, P., Liddell, N., & Jackson, T., 2009. *Certej Updated Definitive Feasibility Study Summary Technical Report*. European Goldfields Limited, 20-36.

Honea, R.M., 1964. *Empressite and stuetzite redefined*. American Mineralogist, 49, 325-338.

Ianovici, V., Borcoș, M., Bleahu, M., Patrulius, D., Lupu, M., Dimitrescu, R., & Savu, H., 1976. *The Geology of Apuseni Mountains (Geologia Munților Apuseni)*, 413-419. (In Romanian).

Karakaya, I., & Thompson, W.T., 1991. T*he Ag-Te (Silver-Tellurium) System.* Journal of Phase Equilibria, 12(1), 56-63.

Kiukkola, K., & Wagner, C., 1957. *Measurements on Galvanic Cells Involving Solid Electrolytes.* Journal of The Electrochemical Society, 104(6), 379.

Kracek, F.C., Ksanda, C.J., & Cabri, L.J., 1966. *Phase relations in the silver-tellurium system* American Mineralogist, 51, 14-28.

Maslennikov, V.V., Maslennikova, S.P., Large, R.R., Danyushevsky, L.V., Herrington, R.J., & Stanley, C.J., 2012. *Tellurium-bearing minerals in zoned sulfide chimneys from Cu-Zn massive sulfide deposits of the Urals, Russia*. Mineralogy and Petrology, 107(1), 67-99.

Milenov, T.I., Tenev, T., Miloushev, I., Avdeev, G.V., Luo, C.W., & Chou, W.C., 2013. *Preliminary studies of the Raman spectra of Ag_2Te Ag_5Te_3.* Optical and Quantum Electronics, 1-8.

Pals, D.W., & Spry, P.G., 2003. T*elluride mineralogy of the low-sulfidation epithermal Emperor gold deposit, Vatukoula, Fiji.* Mineralogy and Petrology, 79(3-4), 285-307.

Pracejus, B., 2008. *The Ore Minerals Under the Microscope: An Optical Guide.* Elsevier Science, 144; 154.

Pricopie, M., Tușa, L., Cristea, P., Căpraru, N., and Marton, I., 2004. *Geology of the Certej project area and a new model for high-grade gold mineralisation hosted within the Dealul Grozii - Hondol Perimeter (Certej deposit).* In C. Ciobanu, N.J. Cook, G. Damian, F. Damian, and G. Buia, Eds. Gold-Silver-Telluride Deposits of the Golden Quadrilateral, South Apuseni Mts., Romania. Guidebook of the International Field Workshop of IGCP project 486, Alba Iulia, Romania, 31st August - 7th September 2004.

Tamas, C.G., Bailly, L., Ghergari, L., O'Connor, G., & Minut, A., 2006. *New Occurrences of Tellurides and Argyrodite in Rosia Montan a, Apuseni Mountains, Romania, and Their Metallogenic Significance.* The Canadian Mineralogist, 44(2), 367-383.

Udubașa, G., Istrate, G., & Vălureanu, M., 1982. *Metallogenesis of Coranda - Hondol region, Metaliferi Mountains (Metalogeneza regiunii Coranda - Hondol, Munții Metaliferi).* (In Romanian). D.S. Inst. Geol., LXVII(2), 197-232.

Udubasa, G., Strusievicz, R.O., Dafin, E., & Verdes, G., 1992. *Mineral occurrences in the Metaliferi Mts., Romania.* Romanian Journal of Mineralogy, 75(2), 1-35.

Udubașa, G. & Udubașa, S.S., 2004. *Au-Ag telluride deposits in the Metaliferi Mts.: effects of local geology or of a "hydrothermal ichor"*. Romanian Journal of Mineral Deposits, 81, Fourth National Symposium of Economic Geology "Gold in Metaliferi Mts.", 39-46.

Xu, H., Yu, Y., Wu, X., Yang, L., Tian, Z., Gao, S. & Wang, Q., 2012. *Intergrowth texture in Au-Ag-Te minerals from Sandaowanzi gold deposit,*

Heilongjiang Province: Implications for ore-forming environment. Chinese Science Bulletin, 57(21), 2778-2786.

Received at: 25. 11. 2013
Revised at: 30. 01. 2014
Accepted for publication at: 10. 02. 2014
Published online at: 19. 02. 2014